


Article

3D Structural Optimization of Zinc Phthalocyanine-Based Sensitizers for Enhancement of Open-Circuit Voltage of Dye-Sensitized Solar Cells

Takuro Ikeuchi ¹, Ryota Kudo ¹, Yu Kitazawa ², Shogo Mori ¹ and Mutsumi Kimura ^{1,2,*} 

¹ Department of Chemistry and Materials, Faculty of Textile Science and Technology, Shinshu University, Ueda 386-8567, Japan; 15st101d@shinshu-u.ac.jp (T.I.); 18fs410j@shinshu-u.ac.jp (R.K.); shogmori@shinshu-u.ac.jp (S.M.)

² Research Initiative for Supra-Materials (RISM), Interdisciplinary Cluster for Cutting Edge Research (ICCER), Shinshu University, Ueda 386-8567, Japan; yu_kitazawa0311@shinshu-u.ac.jp

* Correspondence: mkimura@shinshu-u.ac.jp; Tel.: +81-268-21-5499

Received: 30 March 2020; Accepted: 28 April 2020; Published: 5 May 2020



Abstract: We designed and synthesized two zinc phthalocyanine sensitizers (**PcS27** and **PcS28**), substituted with branched or cyclic alkoxy chains, to investigate the structural effect of peripheral alkyl chains on the performance of dye-sensitized TiO₂ solar cells. The bulky cyclic alkyl chains of **PcS28** decreased the adsorption density of **PcS28** on the TiO₂ electrode, while the terminal branches of alkoxy chains of **PcS27** did not influence the adsorption density in comparison to the previously published **PcS20** with linear alkoxy chains. Under one sun conditions, **PcS27** cells exhibited higher open-circuit voltage but a slightly lower energy conversion efficiency, 6.0% less than **PcS20**. These results suggest that the small alternation of alkoxy chains resulted in decreasing electron pushing ability of peripheral phenoxy units, giving lower short-circuit current.

Keywords: dye-sensitized solar cell; phthalocyanine; open-circuit voltage; branched alkyl chain

1. Introduction

Dye-sensitized solar cells (DSSCs) have drawn special attention as a promising alternative to conventional silicon-based solar cells [1,2]. The solar-to-electronic power conversion efficiency (PCE) of DSSCs has been enhanced by several approaches such as the systematic structural exploration of light-harvesting dyes, the reduction of mismatch between the oxidation potential of the dye and the redox potential of redox couples in electrolyte solutions, and the optimization of the device structures [3]. The light-harvesting dyes, which consist of chromophore units and adsorption sites, play the following three roles: the absorption of light energy, the injection of electrons from the excited dye to the semiconductor electrodes such as TiO₂ and ZnO, and as a barrier to unfavorable contact of redox shuttles with the surface of nanoparticles [4]. Whereas several chromophores with absorption bands in red and near-IR light regions have been applied as light-harvesting dyes for DSSCs, these chromophores have not shown high PCE values. This is partially because of the difficulty of matching HOMO and LUMO energy levels of dyes with two potentials in the DSSC system (the conduction band of the semiconductor electrode and the redox potential of the redox shuttle) [3,5].

Phthalocyanines (Pcs), and especially their metal complexes (MPcs), have been widely used as blue and green dyes and pigments for various applications [6]. The Pcs exhibit intense Q bands in red and near-IR light regions, whose positions can be tuned by the introduction of substituents on the aromatic core and/or modification of central metal species [6]. Thus, the MPcs are good candidates to be the light-harvesting chromophore in DSSCs to harvest red and near-IR light regions. The PCEs of DSSCs sensitized by Pc-based dyes have been improved by several approaches [7–13]. In 2013, we achieved a

PCE of 6.4% from a DSSC employing **PcS20** under one sun conditions [13]. The decoration of short propoxy chains around the Pc core resulted in the formation of a dense adsorption layer of dyes on the surface of TiO₂ without the formation of aggregates. While the incident photon-to-current conversion efficiency (IPCE) at the Q bands for DSSCs based on **PcS20** dye reached 85%, the open-circuit voltage (V_{oc}) (0.60 V) was lower than the reported V_{oc} values for the other dyes because of short electron lifetime in the electrodes of the DSSCs [3]. The attachment of alkyl chains around chromophores has been reported as an effective approach to enhance V_{oc} values in DSSCs [14]. The alkyl chains of sensitizers form a dense barrier layer at the interface of dye-adsorbed TiO₂ surfaces and electrolytes, and the formation of this barrier leads to an increase in electron lifetime. Therefore, further exploration of interfacial engineering for Pc-based dyes is required to achieve high PCE values. In this paper, we examined the structural effect of alkyl chains around the Pc core on the photovoltaic properties.

2. Materials and Methods

General. NMR spectra were recorded on a Bruker AVANCE 400 FT NMR spectrometer at 399.65 MHz and 100.62 MHz for ¹H and ¹³C in CDCl₃ solution. Chemical shifts are reported relative to internal tetramethylsilane. Absorption and fluorescence spectra were measured on a SHIMADZU UV-2600 and a JASCO spectrophotometer FP-8600, respectively. MALDI-TOF mass spectra were obtained on a Bruker Microflex spectrometer with dithranol as the matrix. Mass spectra with electrospray ionization were obtained on a Bruker Daltonics micrOTOF II. Differential pulse voltammetry (DPV) data were recorded with an ALS 720C potentiostat, and electrochemical experiments were performed under purified nitrogen gas. Nanoporous TiO₂ electrodes with 6 μm thickness as the working electrodes of DPV measurements were prepared by applying pastes of TiO₂ nanoparticles with 15–20 nm diameter onto fluoride-doped tin oxide (FTO) glass substrates (Asahi Glass) following sintering at 550 °C for 30 min in air. The TiO₂ electrodes were immersed into 50 μM **PcS27** or **PcS28** solutions in dry toluene for 3 h, and the dye-stained electrodes were used as working electrodes. The reference electrode was Ag/AgCl, which we corrected for junction potentials by referencing it with the ferrocenium/ferrocene (Fc^+/Fc) couple.

All chemicals were purchased from commercial suppliers and used without further purification. Column chromatography was performed with activated alumina (Wako, 200 mesh) or silica gel (Wakogel C-200). Recycling preparative gel permeation chromatography was carried out by a Japan Analytical Industry recycling preparative HPLC using CHCl₃ as an eluent. Analytical thin layer chromatography was performed with commercial Merck plates coated with silica gel 60 F₂₅₄ or aluminum oxide 60 F₂₅₄.

Synthesis of Phthalocyanine Precursors 1 and 2 (Figure 1)

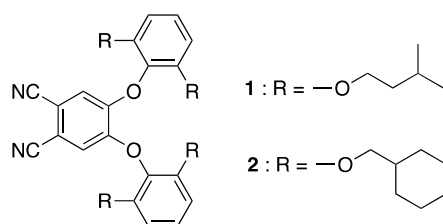


Figure 1. Structure of phthalocyanine precursors 1 and 2.

1: 2,6-(3'-methylbutoxy)phenol [13,15] (0.78 g, 2.9 mmol) and 4,5-dichlorophthalonitrile (0.23 g, 1.2 mmol) were dissolved in 2.0 mL of DMSO. Powder of dried K₂CO₃ (1.23 g, 8.93 mmol) was added to the mixture and stirred at 105 °C for 8 h [12]. After cooling down to room temperature, the reaction mixture was poured into 30 mL of water, and the reaction mixture was extracted with CH₂Cl₂. The combined organic phases were dried over MgSO₄, and the solvent was evaporated. The crude product was purified by silica column chromatography (CH₂Cl₂) and recycling preparative HPLC (CHCl₃) to obtain **1**. Yield 0.42 g (55%). ¹H NMR(CDCl₃, 400.13 MHz): δ/ppm = 7.17 (2H, t, J = 8.4 Hz,

ArH), 6.86 (2H, s, ArH), 6.66 (4H, d, $J = 8.4$ Hz, ArH), 4.01 (8H, t, $J = 6.6$ Hz, $-\text{OCH}_2-$), 1.56 (12H, m, $-\text{CH}_3$), 0.84 (24H, m, $-\text{CH}_3$); ^{13}C NMR (CDCl_3 , 100.61 MHz): $\delta/\text{ppm} = 22.5, 25.1, 37.7, 67.6, 106.5, 108.3, 115.8, 118.1, 126.5, 131.1, 151.3, 152.3$. FT-IR (ATR): $\nu = 2230$ ($-\text{CN}$) cm^{-1} . ESI-TOF HRMS (APCI): m/z 657.4023 $[\text{M} + \text{H}^+]$, calcd. for $\text{C}_{40}\text{H}_{52}\text{N}_2\text{O}_6$: m/z 657.3898.

2: **2** was synthesized from 2,6-bis(cyclohexylmethoxy)phenol (0.74 g, 2.3 mmol) and 4,5-dichlorophthalonitrile (0.18 g, 0.9 mmol) according to the same method as **1**. Yield: 34%. ^1H NMR (CDCl_3 , 400.13 MHz): $\delta/\text{ppm} = 7.13$ (2H, t, $J = 8.8$ Hz, ArH), 6.92 (2H, s, ArH), 6.64 (4H, d, $J = 12.4$ Hz, ArH), 3.76 (8H, d, $J = 6.0$ Hz, $-\text{OCH}_2-$), 1.54–1.69 (24H, m, $-\text{CH}_2-$), 1.18–1.25 (12H, m, $-\text{CH}_2-$), 0.87–0.90 (8H, m, $-\text{CH}_2-$); ^{13}C NMR (CDCl_3 , 100.61 MHz): $\delta/\text{ppm} = 25.6, 26.4, 29.6, 37.4, 74.5, 106.5, 108.2, 119.2, 126.3, 131.5, 151.6, 152.3$. FT-IR (ATR): $\nu = 2231$ ($-\text{CN}$) cm^{-1} . ESI-TOF HRMS (APCI): m/z 761.4724 $[\text{M} + \text{H}^+]$, calcd. for $\text{C}_{48}\text{H}_{60}\text{N}_2\text{O}_6$: m/z 761.4524.

Synthesis of Sensitizers PcS27 and PcS28

PcS27: PcS27 was synthesized from **1** (0.42 g, 0.6 mmol), methyl 3,4-dicyanobenzoate (40 mg, 0.2 mmol), and $\text{Zn}(\text{CH}_3\text{COO})_2$ (59 mg, 0.3 mmol) according to the reported method [12,13]. Yield: 50 mg (10%). UV-Vis in toluene $\lambda_{\text{max}}/\text{nm}$ ($\log \epsilon$): 693 (4.99) and 678 (4.89). ^1H NMR (CDCl_3 , 400.13 MHz): $\delta/\text{ppm} = 10.1$ (br, 1H, COOH), 8.4–8.8 (9H, br, Pc-H), 6.5–7.4 (18H, m, ArH), 4.0–4.1 (24H, m, $-\text{OCH}_2-$), 1.2–1.6 (36H, m, $-\text{CH}_2-$), 0.6 (72H, m, $-\text{CH}_3$). IR (ATR): $\nu = 1681$ ($-\text{COOH}$) cm^{-1} . MALDI-TOF Ms (dithranol): m/z 2206.32 ($\text{M} + \text{H}$), Calcd for $\text{C}_{129}\text{H}_{160}\text{N}_8\text{O}_{20}\text{Zn}$: m/z 2205.12.

PcS28 was synthesized from **2** and methyl 3,4-dicyanobenzoate. Yield: 14%. UV-Vis in toluene $\lambda_{\text{max}}/\text{nm}$ ($\log \epsilon$): 695 (4.94) and 675 (4.90). ^1H NMR (CDCl_3 , 400.13 MHz): $\delta/\text{ppm} = 10.5$ (1H, br, COOH), 8.4–8.7 (9H, br, Pc-H), 6.5–7.4 (18H, m, ArH), 3.7–4.0 (24H, m, $-\text{OCH}_2-$), 1.5–1.7 (72H, m, $-\text{CH}_2-$), 1.1–1.3 (36H, m, $-\text{CH}_2-$), 0.75–0.90 (24H, m, $-\text{CH}_2-$). IR (ATR): $\nu = 1681$ ($-\text{COOH}$) cm^{-1} . MALDI-TOF Ms (dithranol): m/z 2521.38 ($\text{M} + \text{H}$), Calcd for $\text{C}_{153}\text{H}_{184}\text{N}_8\text{O}_{20}\text{Zn}$: m/z 2520.57.

Fabrication of PcS27 and PcS28 DSSC Cells [13]

TiO_2 electrodes (apparent surface area: 0.25 cm^2 ($0.5 \times 0.5 \text{ cm}$)) were printed onto FTO glass substrates by a screen printing technique using two TiO_2 nanoparticle pastes with different diameters of 15–20 and 400 nm. After sintering at 550°C for 30 min in air, the TiO_2 electrodes were treated with TiCl_4 . The **PcS27** or **PcS28** sensitizers were adsorbed onto TiO_2 films by immersion of electrodes in 50 μM toluene solutions of the dyes for 24 h at 25°C . The dye-adsorbed TiO_2 electrode and Pt counter electrode were sealed by heating of a 50 μm thick hot melt ring (Surlyn, DuPont). Redox electrolytes (ELA-1: 0.6 M 1,2-dimethyl-3-propylimidazolium iodide, 0.1 M LiI, 0.05 M I_2 , 0.5 M *tert*-butyl pyridine in acetonitrile) were injected into the space between two electrodes, and then the photovoltaic performance was measured by applying black mask (0.16 cm^2) under a standard AM 1.5 solar condition (100 mW cm^{-2}) with a solar simulator (Otenso-Sun 3SD, Bunko Keiki).

Adsorption Densities of PcS27 and PcS28 on the TiO_2 Surface [12,13]

The adsorption densities of **PcS27** and **PcS28** were determined by measuring the absorbance of dyes released from the TiO_2 electrodes (thickness: 6 μm) by immersing into THF containing tetrabutylammonium hydroxide methanoic solution. The absorbance at the Q band of the released dye was converted into the concentration of dye in the TiO_2 electrode. The adsorption density of dye was calculated from the concentration in the TiO_2 electrode, the surface area of mesoporous TiO_2 ($61 \text{ m}^2/\text{g}$ determined by Brunauer-Emmett-Teller surface area analyzer), and the weight of the TiO_2 electrode on the FTO substrate.

3. Results and Discussion

Two ZnPc-based dyes, **PcS27** and **PcS28**, bearing branched 3-methylbutoxy and cyclic cyclohexylmethoxy chains at the 2 and 6 positions of three peripheral phenoxy units, were designed (Figure 2). We expected the branched and cyclic alkoxy chains to improve the barrier property of the dye monolayer on the TiO₂ surface. Phthalocyanine precursors 1 and 2 were synthesized from resorcinol and 1-bromo-3-methylbutane or (bromomethyl)cyclohexane according to the same procedures as **PcS20** [12,13]. Target ZnPcs **PcS27** and **PcS28** were prepared by a mixed cyclotetramerization between phthalocyanine precursor and methyl 3,4-dicyanobenzoate in the presence of Zn(OAc)₂, and a following hydrolysis [13]. Two ZnPcs and their corresponding intermediates were characterized by using standard spectroscopic techniques.

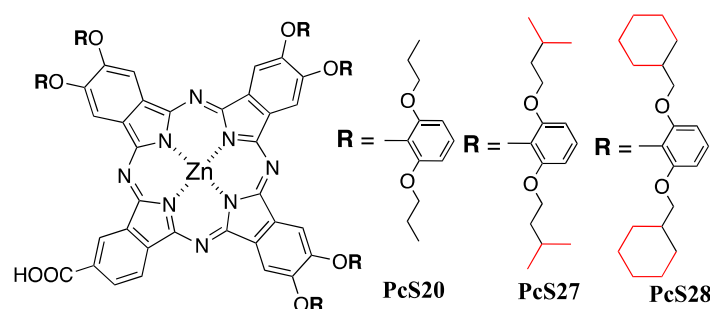


Figure 2. Structure of phthalocyanine sensitizers **PcS20**, **PcS27**, and **PcS28**. Red: structural differences with **PcS20**.

Figure 3a,b shows absorption spectra of **PcS27** and **PcS28** in toluene. The spectrum of **PcS28** exhibited split Q bands at 675 and 695 nm, which were in fair agreement with the previously reported peak positions of **PcS20** [13]. The appearance of split Q bands implies that the degeneracy of LUMO and LUMO+1 energy levels is broken by the asymmetrical substitution of electron-withdrawing carboxylic acid and electron-donating 2,6-dialkoxyphenoxy groups in **PcS28**. The split width between two Q band positions for **PcS27** was narrower than that of **PcS28**. Both ZnPcs emitted a fluorescence at 698 nm upon exciting at the Soret band, indicating that the zero-zero excitation energy (E_{0-0}) obtained by the intersection of the normalized absorption and fluorescence spectra for **PcS27** and **PcS28** was almost the same.

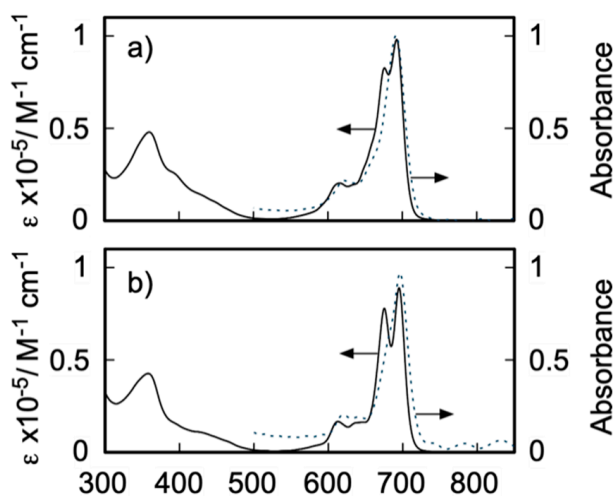


Figure 3. Absorption spectra of **PcS27** (a) and **PcS28** (b) in toluene (solid line) and adsorbed onto TiO₂ film (dotted line).

The TiO₂ electrodes were immersed in toluene solutions of **PcS27** and **PcS28** (50 µM) for 24 hr to give dye-stained TiO₂ electrodes. FT-IR spectra of TiO₂ films stained with **PcS27** or **PcS28** did not show absorption peaks corresponding to carboxylic acid, implying the formation of bidentate binding between carboxylic acid in the dyes and the TiO₂ surface. The absorption spectra of **PcS27** and **PcS28** adsorbed onto TiO₂ films exhibited a single Q band at 692 and 697 nm (Figure 3a,b). The fluorescence emissions from **PcS27** and **PcS28** were quenched on the surface of TiO₂. The absorption spectral changes and fluorescence quenching suggest a good electronic communication between ZnPc and TiO₂ by anchoring carboxylic acid in dyes on the TiO₂. Moreover, the sharp Q bands for both dyes indicate the prevention of molecular aggregation among the ZnPc sensitizers on the TiO₂ surface. The first oxidation potentials (E_{ox}) of **PcS27** and **PcS28** were determined by differential pulse voltammetry measurements using dye-stained TiO₂ electrodes in acetonitrile containing 0.1 M Bu₄NClO₄ as a supporting electrolyte [12]. The E_{ox} values of **PcS27** and **PcS28** were 0.92 and 0.90 V vs. normal standard electrode (NHE), which were attributed to the phthalocyanine ring-based oxidation process. The E_{ox} value of **PcS27** was slightly higher than that of **PcS28** because of the difference in electron-donating properties between 3-methylbutoxy and cyclic cyclohexylmethoxy chains on the peripheral phenoxy units. The E_{ox} values of **PcS27** and **PcS28** are more positive than the potential of the I[−]/I₃[−] redox couple (+0.4 V vs. NHE) [2,16]. Excited oxidation potentials (E_{ox}^*) of **PcS27** and **PcS28** are −0.82 and −0.84 V vs. NHE calculated from E_{ox} and E_{0-0} . The E_{ox}^* values of **PcS27** and **PcS28** are lower than the conduction-band-edge potential of TiO₂ (ca. −0.5 V vs. NHE) [2]. These results suggest that both **PcS27** and **PcS28** dyes possess sufficient potential differences for electron injection from the excited dyes to TiO₂ and the regeneration of the dyes [2].

The DSSC performances of **PcS27** and **PcS28** were conducted using double-layered TiO₂ electrodes with an I[−]/I₃[−] redox electrolyte, ELA-1, under a standard AM 1.5 solar condition (100 mW cm^{−2}). Photocurrent density vs. voltage (J – V) curves are shown in Figure 4a,b. The short-circuit photocurrent density (J_{sc}), V_{oc} , fill factor (FF), and PCE values for the cells sensitized with **PcS27** or **PcS28** are listed in Table 1. The **PcS27** cell exhibited a J_{sc} of 14.1 mA cm^{−2}, a V_{oc} of 610 mV, and an FF of 0.70, yielding a PCE of 6.0%. In contrast, the **PcS28** cell displayed a low PCE value in comparison to the **PcS27** cell. Figure 4c shows the IPCE spectra of **PcS27** and **PcS28** cells. The maximum IPCE values for **PcS27** and **PcS28** cells were 82% and 71% at 600–750 nm corresponding to the Q band of ZnPc sensitizers, and the IPCE spectrum of the **PcS28** cell was narrower than that of the **PcS27** cell. In order to examine the performance difference in the **PcS27** and **PcS28** cells, the adsorption densities of dyes on the TiO₂ surface were determined. The adsorption densities were determined to be 8.2×10^{-11} and 4.9×10^{-11} mol cm^{−2} for **PcS27** and **PcS28**, respectively [17]. The projected molecular area of **PcS27** on the TiO₂ surface calculated from the adsorption density was 2.0 nm², and this value agreed with the area (2.1 nm²) estimated from density functional theory (DFT) and the Corey–Pauling–Koltun (CPK) space-filling model (Figure 5), implying that **PcS27** formed a dense packing layer on the TiO₂ surface. Despite the projected molecular area of **PcS28** (2.1 nm²) being the same as that of **PcS27**, the steric crowding among rigid cyclic cyclohexane side chains in **PcS28** may result in poor packing among dyes on the TiO₂ surface. Therefore, the lower PCE of the **PcS28** cell was due to the lower adsorption density on the TiO₂ surface.

Table 1. Photovoltaic performance of DSSCs sensitized with **PcS27** and **PcS28**.

Dye	Adsorption Density $\times 10^{-11}$ /mol cm ^{−2}	V_{oc} /mV	J_{sc} /mA cm ^{−2}	FF	PCE/%
PcS27	8.2	610	14.1	0.70	6.0
Pcs28	4.9	590	9.3	0.74	4.1

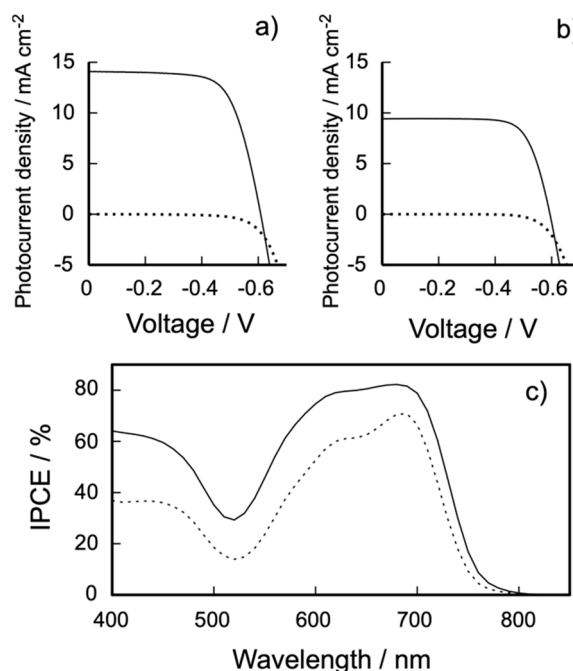


Figure 4. Photocurrent–voltage curves obtained with dye-sensitized solar cells (DSSCs) based on **PcS27** (a) and **PcS28** (b) under a standard global AM 1.5 solar condition (solid line) and darkness (dashed line); (c) incident photon-to-current conversion efficiency spectra for DSSCs based on **PcS27** (solid line) and **PcS28** (dashed line).

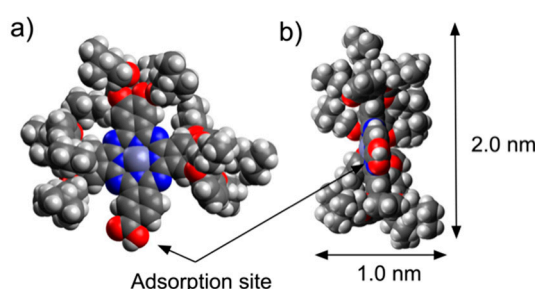


Figure 5. Corey–Pauling–Koltun (CPK) model of **PcS27** ((a) top view; (b) side view) calculated by Gaussian 16.

Since there is no difference in adsorption density between **PcS27** and our previously reported **PcS20** decorated with linear propoxy chains [13], the branching terminal units do not influence the packing density on the surface of TiO₂. The V_{oc} value of the **PcS27** cell was 10 mV higher than that of the **PcS20**, and the offset potential of dark current of the **PcS27** cell was higher than that of the **PcS20** cell. This suggests that covering the ZnPc core with branched alkyl chains in **PcS27** may retard the interfacial charge recombination from the conduction band of TiO₂ to I₃[−]. The narrower split width of the Q band and the higher E_{ox} for **PcS27** revealed the poor electron-pushing ability of peripheral units as compared to **PcS20**. This poor electron-pushing ability of **PcS27** relative to **PcS20** leads to the inferior J_{sc} and IPCE values in DSSCs.

4. Conclusions

The performances of DSSCs based on ZnPcs decorated with branched or cyclic alkoxy chains at the peripheral phenoxy units were examined. The **PcS27** cell with 3-methylbutoxy chains showed 6.0% efficiency when used as a light-harvesting sensitizer on a TiO₂ electrode under one sun conditions. We found that the terminal branches of alkoxy chains did not influence the adsorption density on the TiO₂ surface, and the **PcS27** cell exhibited a higher V_{oc} value than the **PcS20** with linear alkoxy

chains. The obtained V_{oc} value of the **PcS27** cell was still lower than the potential difference (0.9 V) between the conduction-band-edge potential of TiO_2 and the redox potential of the I^-/I_3^- redox shuttle. The covering of the ZnPc core with alkyl chains should be effective to prevent unfavorable charge recombination. However, the excess decoration of the ZnPC core with alkyl chains leads to a decrease in the adsorption density of sensitizers on the TiO_2 surface. The achievement of high V_{oc} values for ZnPc-based DSSCs requires further substituent design of a large π -surface of the ZnPc core to enhance the blocking function to the approach of I_3^- in electrolytes, while keeping high adsorption density on the TiO_2 surface.

Author Contributions: All authors contributed equally. M.K. and S.M. conceived the original idea and guided the project. M.K. designed sensing materials and wrote the manuscript. T.I., R.K., and Y.K. carried out dye synthesis, characterization, and fabrication of DSSCs. All authors assisted with the manuscript preparation and discussed the results. All authors have read and agreed to the published version of the manuscript.

Funding: This work has been partially supported by Grants-in-Aid for Scientific Research (A) (No. 15H02172) and (B) (No. 17H03099) from the Japan Society for the Promotion of Science (JSPS) of Japan.

Conflicts of Interest: The authors declare no conflict of interest.

References

- O'Regan, B.; Grätzel, M. A low-cost, high-efficiency solar cell based on dye-sensitized colloidal TiO_2 films. *Nature* **1991**, *353*, 737–740. [\[CrossRef\]](#)
- Grätzel, M. Photoelectrochemical cells. *Nature* **2001**, *414*, 338–344. [\[CrossRef\]](#) [\[PubMed\]](#)
- Hagfeldt, A.; Boschloo, G.; Sun, L.; Kloo, L.; Pettersson, H. Dye-sensitized solar cells. *Chem. Rev.* **2010**, *110*, 6595–6663. [\[CrossRef\]](#) [\[PubMed\]](#)
- Robertson, N. Optimizing dyes for dye-sensitized solar cells. *Angew. Chem. Int. Ed.* **2006**, *45*, 2338–2345. [\[CrossRef\]](#) [\[PubMed\]](#)
- Qin, C.; Numata, Y.; Zhang, S.; Yang, X.; Islam, A.; Zhang, K.; Chen, H.; Han, L. Novel near-infrared squaraine sensitizers for stable and efficient dye-sensitized solar cells. *Adv. Funct. Mater.* **2014**, *24*, 3059–3066. [\[CrossRef\]](#)
- De la Torre, G.; Claessens, C.G.; Torres, T. Phthalocyanines: Old dyes, new materials. Putting color in nanotechnology. *Chem. Commun.* **2007**, *28*, 2000–2015. [\[CrossRef\]](#) [\[PubMed\]](#)
- Reddy, P.Y.; Giribabu, L.; Lyness, C.; Snaith, H.J.; Vijaykumar, C.; Chandrasekharam, M.; Lakshmikantham, M.; Yum, J.-H.; Kalyanasundaram, K.; Grätzel, M.; et al. Efficient sensitization of nanocrystalline TiO_2 films by a near-IR-absorbing unsymmetrical zinc phthalocyanine. *Angew. Chem. Int. Ed.* **2007**, *46*, 373–376. [\[CrossRef\]](#) [\[PubMed\]](#)
- Cid, J.-J.; Yum, J.-H.; Jang, S.-R.; Nazeeruddin, M.K.; Martínez-Ferro, E.; Palomares, E.; Ko, J.; Grätzel, M.; Torres, T. Molecular cosensitization for efficient panchromatic dye-sensitized solar cells. *Angew. Chem. Int. Ed.* **2007**, *46*, 8358–8362. [\[CrossRef\]](#) [\[PubMed\]](#)
- Mori, S.; Nagata, M.; Nakahata, Y.; Yasuta, K.; Goto, R.; Kimura, M.; Taya, M. Enhancement of incident photon-to-current conversion efficiency for phthalocyanine-sensitized solar cells by 3D molecular structuralization. *J. Am. Chem. Soc.* **2010**, *132*, 4054–4055. [\[CrossRef\]](#) [\[PubMed\]](#)
- Kimura, M.; Nomoto, H.; Masaki, N.; Mori, S. Dye molecules for simple co-sensitization process: Fabrication of mixed-dye-sensitized solar cells. *Angew. Chem. Int. Ed.* **2012**, *51*, 4371–4374. [\[CrossRef\]](#) [\[PubMed\]](#)
- Ragoussi, M.-E.; Cid, J.-J.; Yum, J.-H.; de la Torre, G.; Di Censo, D.; Grätzel, M.; Nazeeruddin, M.K.; Torres, T. Carboxyethynyl anchoring ligands: A means to improving the efficiency of phthalocyanine-sensitized solar cells. *Angew. Chem. Int. Ed.* **2012**, *51*, 4375–4378. [\[CrossRef\]](#) [\[PubMed\]](#)
- Kimura, M.; Nomoto, H.; Suzuki, H.; Ikeuchi, T.; Matsuzaki, H.; Murakami, T.N.; Furube, A.; Masaki, N.; Griffith, M.J.; Mori, S. Molecular design rule of phthalocyanine dyes for highly efficient near-IR performance in dye-sensitized solar cells. *Chem. Eur. J.* **2013**, *19*, 7496–7502. [\[CrossRef\]](#) [\[PubMed\]](#)
- Ikeuchi, T.; Nomoto, H.; Masaki, N.; Griffith, M.J.; Mori, S.; Kimura, M. Molecular engineering of zinc phthalocyanine sensitizers for efficient dye-sensitized solar cells. *Chem. Commun.* **2014**, *50*, 1941–1943. [\[CrossRef\]](#) [\[PubMed\]](#)

14. Koumura, N.; Wang, Z.-S.; Mori, S.; Miyashita, M.; Hara, K. Alkyl-functionalized organic dyes for efficient molecular photovoltaics. *J. Am. Chem. Soc.* **2006**, *128*, 14256–14257. [[CrossRef](#)] [[PubMed](#)]
15. Yella, A.; Lee, H.-W.; Tsao, H.N.; Yi, C.; Chandiran, A.K.; Nazeeruddin, M.K.; Díau, E.W.-G.; Yeh, C.-Y.; Zakeeruddin, S.M.; Grätzel, M. Protophyrin-sensitized solar cells with cobalt (II/III)-based redox electrolyte exceed 12 percent efficiency. *Science* **2011**, *334*, 629–634. [[CrossRef](#)] [[PubMed](#)]
16. Wu, J.; Lan, Z.; Lin, J.; Huang, M.; Huang, Y.; Fan, L.; Luo, G. Electrolytes in dye-sensitized solar cells. *Chem. Rev.* **2015**, *115*, 2136–2173. [[CrossRef](#)] [[PubMed](#)]
17. Imahori, H.; Matsubara, Y.; Iijima, H.; Uneyama, T.; Matano, Y.; Ito, S.; Niemi, M.; Tkachenko, N.V.; Lemmetyinen, H. Effects of *meso*-diarylamino group of porphyrins as sensitizers in dye-sensitized solar cells on optical, electrochemical, and photovoltaic properties. *J. Phys. Chem. C* **2010**, *114*, 10656–10665. [[CrossRef](#)]



© 2020 by the authors. Licensee MDPI, Basel, Switzerland. This article is an open access article distributed under the terms and conditions of the Creative Commons Attribution (CC BY) license (<http://creativecommons.org/licenses/by/4.0/>).